International Journal of Chronic Obstructive Pulmonary Disease

Dovepress
Taylor & Francis Group

Open Access Full Text Article

ORIGINAL RESEARCH

Upregulation of ARHGAP18 by miR-613 Inhibits Cigarette Smoke Extract-Induced Apoptosis and Epithelial-Mesenchymal Transition in Bronchial Epithelial Cells

Haifan Fu[1,2,*], Kai Liu[3,*], Yamei Zheng[3], Jie Zhao[3], Tian Xie[3], Yipeng Ding[2,3]

[1]Yangjiang Health Center of Qionghai County, Qionghai, Hainan Province, People's Republic of China; [2]Department of General Practice, Hainan Affiliated Hospital of Hainan Medical University, Hainan General Hospital, Haikou, People's Republic of China; [3]Department of Pulmonary and Critical Care Medicine, Hainan General Hospital, Hainan Affiliated Hospital of Hainan Medical University, Haikou, People's Republic of China

*These authors contributed equally to this work

Correspondence: Yipeng Ding, Hainan General Hospital, No. 19, Xinhua Road, Xiuying District, Haikou, 570311, Hainan, People's Republic of China, Tel +86 18976335858, Email ypding1961@163.com

Objective: Chronic Obstructive Pulmonary Disease (COPD) is a major chronic respiratory disease affecting human health worldwide. However, there is still a lack of effective drugs for treating COPD. This study is intended to explore the function and molecular mechanism of *ARHGAP18* and miR-613 in COPD pathogenesis.

Methods: We initially identified the marker gene closely related to epithelial dysfunction in COPD by integrating bioinformatic analyses. *ARHGAP18* expression in CSE-induced bronchial epithelial cells (BEAS-2B) was detected by qRT-PCR. Besides, *ARHGAP18* levels were modulated by lentivirus-mediated overexpression. Thereafter, cell variability, apoptosis, and migration were detected by CCK8, flow cytometry, and wound healing assay. IL-1β and TNF-α levels were examined by qRT-PCR. Epithelial-mesenchymal transition (EMT)-associated proteins were determined by Western blotting. The function of miR-613 in COPD was further detected. Functional rescue experiments were performed to determine the mechanism of *ARHGAP18* in COPD.

Results: Our study identified *ARHGAP18* as the key gene associated with epithelial dysfunction in COPD. *ARHGAP18* was downregulated in CSE-induced BEAS-2B cells. Overexpression of *ARHGAP18* inhibited cell apoptosis of BEAS-2B cells and enhanced their proliferation and migration. Besides, *ARHGAP18* overexpression reduced IL-1 β and TNF-α levels, enhanced E-cadherin expression, and suppressed Vimentin and N-cadherin expression. In contrast, miR-613 mimics exerted opposite effects. Furthermore, downregulation of *ARHGAP1*, mediated by miR-613 inhibitor promoted cell apoptosis and EMT of CSE-induced BEAS-2B cells, suggesting a regulatory role of miR-613 in COPD pathogenesis.

Conclusion: These findings highlight miR-613/*ARHGAP18* axis as a critical regulator of epithelial dysfunction in COPD, offering a potential therapeutic target to counteract apoptosis, inflammation, and airway remodeling.

Keywords: chronic obstructive pulmonary disease, *ARHGAP18*, apoptosis, epithelial-mesenchymal transition, miR-613

Introduction

Chronic Obstructive Pulmonary Disease (COPD) is a common chronic respiratory disease characterized by continuous airflow restriction. Its clinical manifestations are cough, expectoration, wheezing, and dyspnea, which seriously affect patients' quality of life and longevity.[1] Globally recognized as the third leading cause of death, COPD affects approximately 384 million people, with disease burden strongly linked to population aging, smoking prevalence, and environmental pollution.[1,2] In China, COPD demonstrates a prevalence rate of 8.6%, impacting over 100 million adults aged 40 and above. Despite this substantial disease burden, diagnostic rates remain below 30%, leaving millions untreated and contributing to a critical public health challenge termed the "hidden epidemic of undiagnosed

Received: 24 February 2025
Accepted: 19 June 2025
Published: 18 July 2025

patients".[3,4] The pathogenesis of COPD is complicated, involving chronic inflammation, oxidative stress, apoptosis, and other pathophysiological processes.[5] Despite progress in the diagnosis and treatment of COPD, its global morbidity and mortality remain high. This is especially evident in developing countries like China, where the disease burden is particularly severe.[4] Due to the heterogeneity of COPD, its pathogenesis has not been fully clarified, bringing significant challenges to the development of precision treatment strategies.[6] While bronchodilators and anti-inflammatory drugs are the main drugs for current COPD management, substantial variability exists in patients' therapeutic responses, and some patients even develop drug tolerance.[7] It is very important to determine COPD pathogenesis in depth to explore new biomarkers and drug treatment strategies.

Cigarette smoke (CS), the predominant COPD risk factor, induces airway epithelial injury through oxidative stress and inflammatory cascades. Emerging evidence highlights epithelial-mesenchymal transition (EMT) as a critical process in CS-induced airway remodeling. Clinical studies demonstrate that EMT markers (eg, vimentin upregulation and E-cadherin loss) correlate with disease severity and accelerated lung function decline in COPD patients.[8] Mechanistically, Wei et al showed that CS promoted bronchial epithelial cells' EMT by activating STAT3/PINK1 signaling pathway.[9] Further research indicates that CS aggravates EMT and promotes airway inflammation and fibrosis by influencing PINK1/Parking-mediated mitophagy.[10]

In our preliminary research, we observed that three downregulated genes (including *ARHGAP18, AGR3*, and FGG) were closely related to epithelial cells in COPD through multiple bioinformatic analyses. The functions of *AGR3* and *FGG* in COPD have been extensively studied in previous research.[11,12] Thus, this study determined the functions of *ARHGAP18* in COPD. *ARHGAP18*, a Rho GTPase-activating protein (RhoGAP), contributes to cytoskeleton remodeling, cell polarity, and wound repair in epithelial cells. Lombardo et al demonstrated that ARHGAP18 regulates actin structure formation in epithelial cells and is essential for maintaining cell polarity and barrier function.[13] Additionally, Coleman et al revealed that *ARHGAP18* acts in concert with the YAP signaling pathway to regulate endothelial cell alignment under fluid shear stress.[14] The functions of *ARHGAP18* in COPD have not been unexplored. Thus, we conducted this study to determine the biological functions of *ARHGAP18* in COPD.

MicroRNAs (miRNAs), small non-coding RNA molecules, modulate target genes' expression by inhibiting mRNA translation or promoting its degradation.[15] Studies have demonstrated that miRNAs play critical regulatory roles in initiation, progression, and resolution. This regulation is often mediated by positive and negative feedback mechanisms, particularly in inflammatory lung diseases.[16] miR-613 is a multifunctional microRNA with broad regulatory roles, exerting critical effects across various diseases by targeting distinct signaling molecules. In oncology, it suppresses renal cell carcinoma proliferation, invasion, and migration through inhibition of the AXL/AKT pathway,[17] while impeding malignant progression in papillary thyroid carcinoma by targeting TAGLN2.[18] Notably, miR-613 significantly reduces chemoresistance and tumor stemness in triple-negative breast cancer via modulation of FAM83A, offering novel strategies to overcome therapeutic resistance.[19] Beyond oncological contexts, miR-613 plays essential physiological regulatory roles, exemplified by its maintenance of proliferation-differentiation balance in ovarian granulosa cells through IGF-1 targeting and subsequent cell cycle regulation.[20] Moreover, the expression of miR-613 is significantly reduced in non-small cell lung cancer, and this reduction enhances the proliferation and migration of tumor cells.[21] However, the impact of miR-613 on COPD remains unclear.

In the current study, the abnormal mRNA related to COPD was predicted by using public bioinformatic databases and machine learning methods, and specific mRNA was screened out. We identified *ARHGAP18* as being closely associated with COPD and further investigated its biological functions and molecular mechanism in COPD using a CSE-induced human bronchial epithelial cells (BEAS-2B) cell model.

Materials and Methods

Bioinformatic Analysis

To validate findings linked to bronchial epithelial cells in COPD, we analyzed four GEO datasets (GSE76925, GSE47460, GSE167295, and GSE24709) with clinical relevance to COPD pathogenesis. The GSE76925 dataset (111 COPD vs 40 controls, lung tissue, GPL10558) was conducted using the R package "limma" to identify differentially

expressed genes (DEGs), with the screening criteria of an adjusted p-value < 0.05 and a log2 fold change> 1. The GSE24709 dataset (24 COPD vs 19 controls, blood profiles, GPL9040) was analyzed similarly to screen COPD-associated miRNAs. Single-cell RNA-seq data (GSE167295, GPL18573) were normalized and annotated via "Seurat" and "SingleR" to identify epithelial subpopulation markers. Key hub genes were prioritized by integrating LASSO, Random Forest (RF), and Linear Discriminant Analysis-Recursive Feature Elimination (LDA-RFE) algorithms. Finally, the GSE47460 dataset (205 COPD vs 63 controls, lung tissue, GPL6480) independently validated hub gene expression differences.

Cell Culture and Treatment

BEAS-2B cells were purchased from Wuhan Punosai Life Technology Co., LTD. Cells were cultured in DMEM medium containing 10% FBS and 1% penicillin/streptomycin at 37 °C and 5% CO_2. BEAS-2B cells were treated with CSE of 0.0%, 1.0%, 2.5%, 5.0%, 7.5%, 10.0%, and 25.0% for 24 hours. At the end of the treatment, the CCK-8 mixture was replaced and the incubation was continued for 4 h. The absorbance value was determined at a wavelength of 450 nm.

Preparation of CSE

CSE was prepared using the suction mechanism of the standard human smoking pattern of 30 mL/mouth, 2 seconds/mouth, and 1 mouth/minute, and the method was referred to previously reported[22] with slight modifications as described in our previous work.[23]

Cell Transfection

Before transfection, 2×10^5 cells were plated into 6-well dishes with 2 mL of antibiotic-free medium. A transfection procedure was initiated once the cells attained 60% to 80% confluency. miR-163 inhibitor, miR-163 mimic, siARHGAP18, and LV5-ARHGAP18 were synthesized by Gemma Pharmaceutical Co., LTD. The sequences were subsequently transfected into the cell lines using Lipofectamine 2000 reagent, following the manufacturer's protocol.

Cell Viability and Cell Apoptosis Assays

To assess cell viability, normal or transfected cells were plated in 96-well plates at 2×10^4 cells/well. After adding 10 μL of CCK-8 reagent (InCellGene, Beijing, China) to each well, the plates were incubated at 37°C for 2 hours, and absorbance was measured at 450 nm using a microplate reader. For cell apoptosis, normal or transfected cells were plated in 6-well plates at 1×10^5 cells/well and cultured for 24 hours at 37°C with 5% CO_2. After washing with PBS, cells were centrifuged and resuspended in 1% BSA. And treated with Muse Annexin V & Dead Cell reagent (Luminex, USA). Following a 20-minute dark incubation, samples were analyzed using flow cytometry (Muse, USA).

Wound Healing Assay

Cells were cultured in 6-well plates until they reached 90% confluence. A scratch was created on the monolayer using the tip of a 20 μL micropipette. After scratching, the cells were rinsed gently with PBS to remove exfoliated cells and then maintained in a DMEM medium with 10% FBS. Photographs were taken at 0 h and 24 h after scratch, and the width of wound healing was observed and recorded using a microscope.

qRT-PCR Analysis

Total RNA was extracted from BEAS-2B cells using Trizol reagent (Agbio, Hunan, China). The RNA concentration and quality were quantified by measuring the absorbance at 260 nm with a NanoDrop 2000 spectrophotometer. Subsequently, high-quality RNA was reverse transcribed into cDNA using the NovoScript Plus First-Strand cDNA Synthesis SuperMix. qRT-PCR analysis was performed on an ABI 7500 real-time PCR system (ABI, USA), using SYBR High Sensitivity qPCR SuperMix (Novoprotein, Suzhou, China). The primer sequences are shown in Table S1. The target genes' relative expression levels were determined using the 2^-ΔΔCt method.

Western Blot Assay

Total proteins were extracted from BEAS-2B cells using RIPA buffer supplemented with protease inhibitors, and their concentrations were measured by the BCA method. The protein samples were separated by 10% SDS-PAGE and transferred to PVDF membranes by semi-dry electrophoresis. The membranes were blocked using 5% skim milk for 2 hours at room temperature, followed by overnight incubation with primary antibodies at 4 °C. After washing three times with TBST, they were treated with secondary antibodies for 1 hour at room temperature and washed thrice. Finally, the membranes were developed with ECL reagent and imaged on the E-BLOT system.

Luciferase Reporter Assay

The 3′-UTR fragment of wild-type or mutant *ARHGAP18* was inserted into the pmirGLO vector, which was then co-transfected into 293T cells alongside miR-613 mimics or negative control (NC mimics). After transfection, luciferase activity was measured using a dual luciferase reporter assay kit (GENE CREATE, China) to evaluate the binding of miR-613 with *ARHGAP18*.

Statistical Analyses

Statistical analysis was performed using GraphPad Prism 9.0 software. All experiments were repeated independently three times, and the data were expressed as mean ± standard deviation (SD). One-way ANOVA was applied for multi-group comparisons, with statistical significance set as $p< 0.05$.

Results

ARHGAP18 Is a Novel Gene Associated with COPD

To identify the genes associated with COPD, we first analyzed the gene expression microarray data of the GSE76925 dataset. Figure 1A reveals 460 differentially expressed genes (DEGs), comprising 413 downregulated and 47 upregulated genes. Subsequently, we preprocessed scRNA-seq data. As shown in Figure 1B, the t-SNE plot demonstrates the distribution of different clusters, and the cell annotation of these clusters. Using the "FindAllMarkers" function (logFC≥ 0.5, $p< 0.05$) to analyze highly variable genes in each cluster, 625 marker genes specific to epithelial cell clusters were identified (Table S1). The intersection of the DEGs and the 625 genes obtained from single-cell sequencing was taken, and ultimately, 9 candidate genes were selected (Figure 1C).

To further screen the key genes, we analyzed these 9 genes using three machine learning algorithms: LASSO, RF, and LDA-RFE, and the results are shown in Figure 1D–F. By taking the intersection of the genes obtained from the three algorithms, we ultimately identified 5 key genes: *ADI1, ARHGAP18, MLF1, AGR3*, and *FGG* (Figure 1G). Subsequently, we verified these genes' expression levels using the GSE47460 dataset. As shown in Figure 1H, *ARHGAP18, AGR3*, and *FGG* were significantly downregulated in COPD. Since *AGR3* and *FGG* have been extensively studied in previous research, this study chose *ARHGAP18* for subsequent functional studies.

ARHGAP18 Expression Is Downregulated in CSE-Induced BEAS-2B Cells

To establish a bronchial epithelial inflammatory cell model, BEAS-2B cells were induced by CSE. Firstly, the cell viability was evaluated by CCK-8. As shown in Figure 2A, the cells treated with 10% and 25% CSE showed obvious toxic reactions, so the concentrations of 5.0% and 7.5% CSE were selected for further study in subsequent experiments. Subsequently, the effect of CSE on cell apoptosis was analyzed by the Muse cell apoptosis assay (Figure 2B). Compared to the control group, 7.5% CSE significantly increased cell apoptosis ($p< 0.01$). Furthermore, qRT-PCR was used to measure inflammatory factor levels in treated cells, as illustrated in Figure 2C. After 7.5% CSE treatment, IL-1β and TNF-α levels were notably enhanced ($p< 0.01$). In conclusion, 7.5% CSE was chosen as the best treatment concentration for constructing the bronchial epithelial inflammatory cell model. Finally, we examined *ARHGAP18* expression in CSE-induced BEAS-2B cells, and *ARHGAP18* was significantly reduced in CSE-treated cells ($p< 0.001$, Figure 2D).

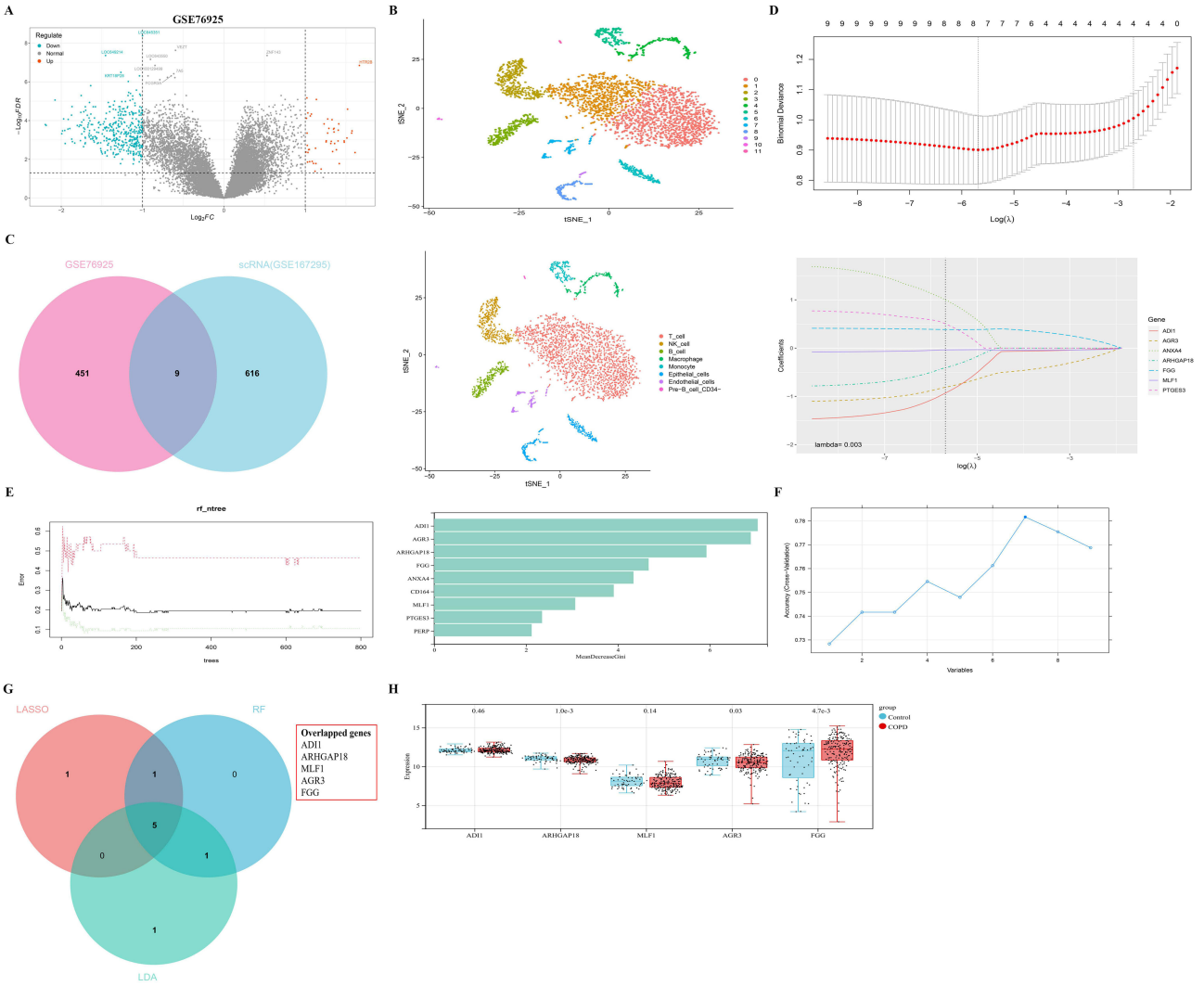

Figure 1 *ARHGAP18* was an epithelial cell-specific gene in COPD. (**A**) Volcano plot of differentially expressed genes in COPD. The analysis was based on GSE76925 dataset, which includes 111 COPD patients and 40 controls. Red and blue dots represent up-regulated and downregulated genes, respectively. The gray dots indicate non-differentially expressed genes. The cutoff values were set as logFC> 1 or < −1 and adjusted *p*-value< 0.05. (**B**) The tSNE plot shows the distribution of different clusters and their corresponding cell annotations. The analysis was performed on the GSE76925 dataset from single-cell RNA-seq data. The plot illustrates the distribution of various cell types, including epithelial cells, macrophages, T cells, etc. Each point represents a single cell, and the colors correspond to different cell types as indicated in the legend. (**C**) Overlap genes of GSE76925 dataset and scRNA dataset. (**D**) Variables were screened by LASSO regression analysis based on the GSE76925 dataset. The plot shows the coefficient profiles of the variables (genes) during the LASSO regression process. The optimal lambda value was chosen as 0.003, and the corresponding variables were selected for further analysis. (**E**) Genes were ranked by importance using a random forest algorithm. The plot shows the importance scores of the top genes. The higher the score, the more important the gene is in distinguishing COPD samples from normal samples. (**F**) Genes were identified through SVM-RFE. The plot shows the accuracy of the model during the recursive feature elimination process. The genes were ranked according to their contribution to the classification accuracy. (**G**) The intersection of key genes was screened by the three methods. (**H**) The expression of the key genes was validated in the GSE47460 dataset (205 COPD patients and 63 controls). The box plots show the expression levels of these genes in COPD patients and normal controls. The error bars represent the standard deviation, and the *p*-values were calculated using *t*-test. The *p*-value thresholds were set as 0.05.

Overexpression of ARHGAP18 Inhibits Inflammatory Response and Epithelial-Mesenchymal Transition in CSE-Treated BEAS-2B Cells

To explore the biological function of *ARHGAP18*, we constructed a cell line that stably overexpressed *ARHGAP18* by transfection into BEAS-2B cells with lentivirus. Transfection efficiency was verified through Western blotting and qRT-PCR. Figure 3A shows that LV5-ARHGAP18 markedly elevated *ARHGAP18* expression level. Subsequently, we detected the impact of *ARHGAP18* overexpression on apoptosis using flow cytometry. The results showed that LV5-ARHGAP18 in the CSE+LV5-*ARHGAP18* group significantly reduced CSE-induced apoptosis in BEAS-2B cells compared to the CSE group (Figure 3B). CCK8 analysis further confirmed that overexpression of *ARHGAP18*

 https://doi.org/10.2147/COPD.S524723

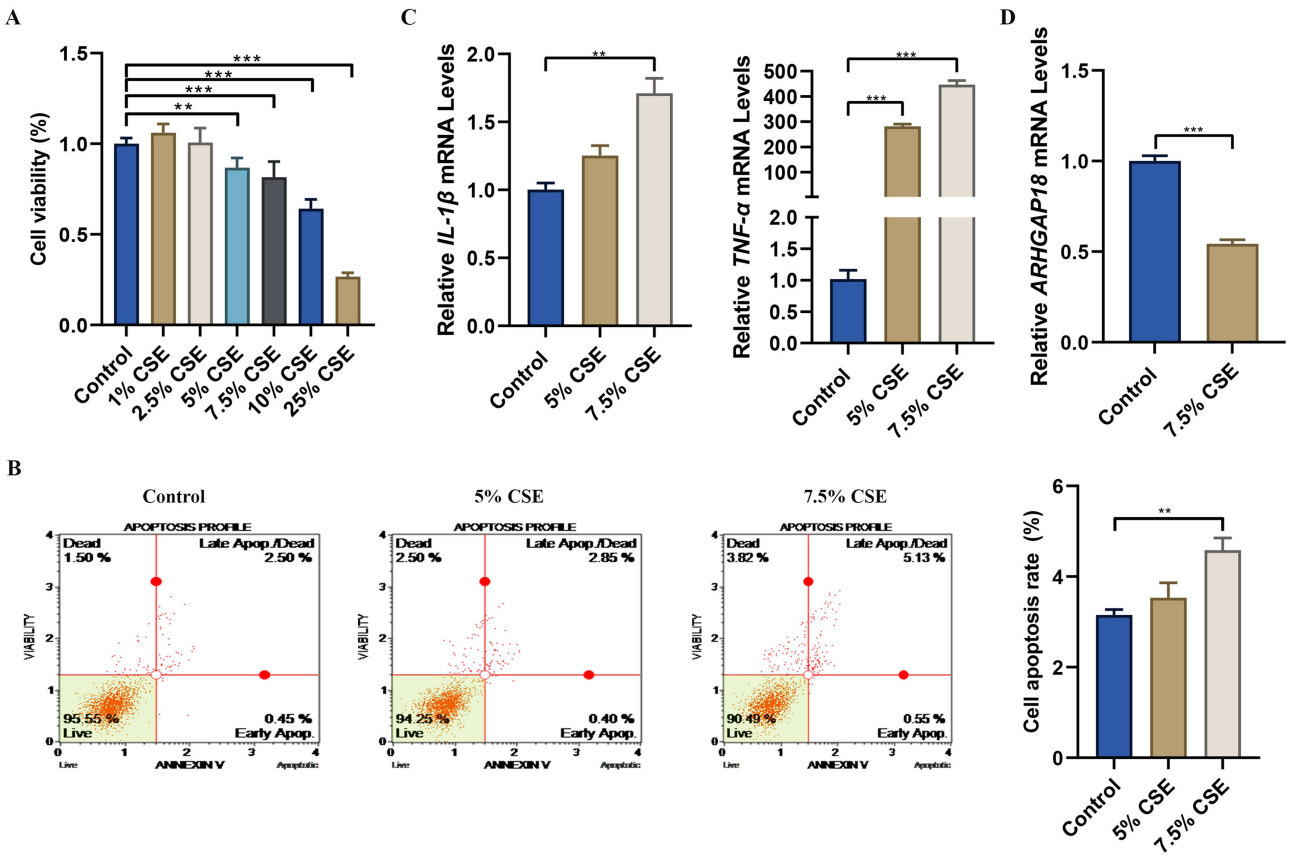

Figure 2 *ARHGAP18* was downregulated in CSE-induced BEAS-2B cells. (**A**) Cell viability was assessed by CCK8 assay in BEAS-2B cells treated with different concentrations of CSE. (**B**) Cell apoptosis was examined using flow cytometry in BEAS-2B cells with CSE treatment. (**C**) The expression levels of IL-1β and TNF-α were examined by qRT-PCR in CSE-induced BEAS-2B cells. (**D**) The expression of ARHGAP18 was detected by qRT-PCR in CSE-induced BEAS-2B cells. The results are presented as the mean ± SD of three independent experiments (n= 3). One-way ANOVA was applied for multi-group comparisons, with statistical significance set as $p< 0.05$. **: $p< 0.01$, and ***: $p< 0.0001$.

dramatically promoted CSE-induced proliferation in BEAS-2B cells (Figure 3C). The wound healing test revealed that LV5-ARHGAP18 significantly enhanced cell migration compared to the CSE group (Figure 3D). In addition, we also detected the expression levels of inflammatory factors, and the results showed that the overexpression of *ARHGAP18* significantly inhibited IL-1β and TNF-α expressions compared with the CSE group (Figure 3E). To further explore the mechanism of *ARHGAP18*, we examined EMT-related protein expression by Western blotting. Figure 3F revealed that *ARHGAP18* overexpression was able to increase E-cadherin while inhibiting N-cadherin and Vimentin.

miR-613 Mediates ARHGAP18 Suppression and Promotes Inflammation and EMT in BEAS-2B Cells with CSE Treatment

To determine whether microRNAs (miRNAs) are involved in *ARHGAP18* expression regulation in CSE-induced BEAS-2B cells, we first screened the differentially expressed miRNAs through the GSE 24709 dataset. As shown in Figure 4A, 90 differentially up-regulated miRNAs were screened out. Next, we performed bioinformatics analysis using miRDB and Starbase to predict the potential miRNAs that might regulate *ARHGAP18*, respectively. By taking the intersection of the above results, we obtained 2 upregulated miRNAs, namely hsa-miR-206 and hsa-miR-613 (Figure 4B). Since miR-206 has been extensively reported in the literature, we selected miR-613 as a potential regulatory target of *ARHGAP18*.

To verify the binding of miR-613 to *ARHGAP18*, a luciferase reporter assay was performed. As shown in Figure 4C, miR-613 and *ARHGAP18* did have a binding interaction. Subsequently, we analyzed miR-613 expression in CSE-induced BEAS-2B cells by RT-PCR, and miR-613 was upregulated in CSE-treated BEAS-2B cells (Figure 4D). We further transferred miR-613 mimics into BEAS-2B cells, and qRT-PCR analysis revealed a significant increase in miR-

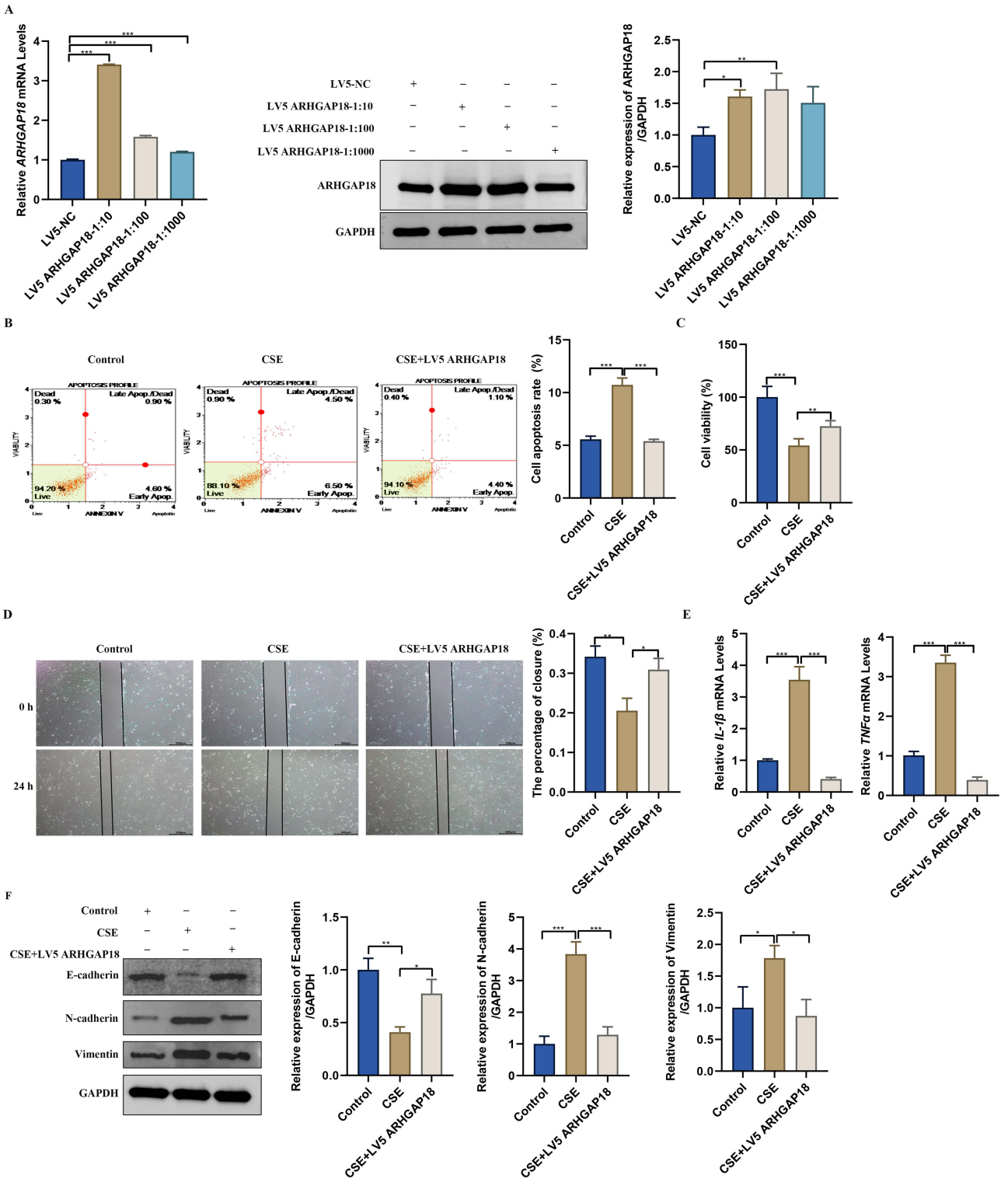

Figure 3 Overexpression of *ARHGAP18* inhibited cell apoptosis and EMT and enhanced proliferation and migration of BEAS-2B cells in vitro. (**A**) Overexpression efficiency of *ARHGAP18* in BEAS-2B cells was detected by qRT-PCR and Western blotting. (**B**) The effect of *ARHGAP18* overexpression on the apoptosis of BEAS-2B was detected by flow cytometry. (**C**) CCK8 was performed to assess the influence of *ARHGAP18* overexpression on the cell viability of BEAS-2B. (**D**) The impact of *ARHGAP18* overexpression on the migration of BEAS-2B was detected by wound healing assay. (**E**) The levels of IL-1β and TNF-α were measured by qRT-PCR. (**F**) The levels of E-cadherin, N-cadherin, and Vimentin were measured by Western blotting. The results are presented as the mean ± SD of three independent experiments (n= 3). One-way ANOVA was applied for multi-group comparisons, with statistical significance set as $p< 0.05$. *: $p< 0.05$, **: $p< 0.01$, and ***: $p< 0.0001$.

https://doi.org/10.2147/COPD.S524723

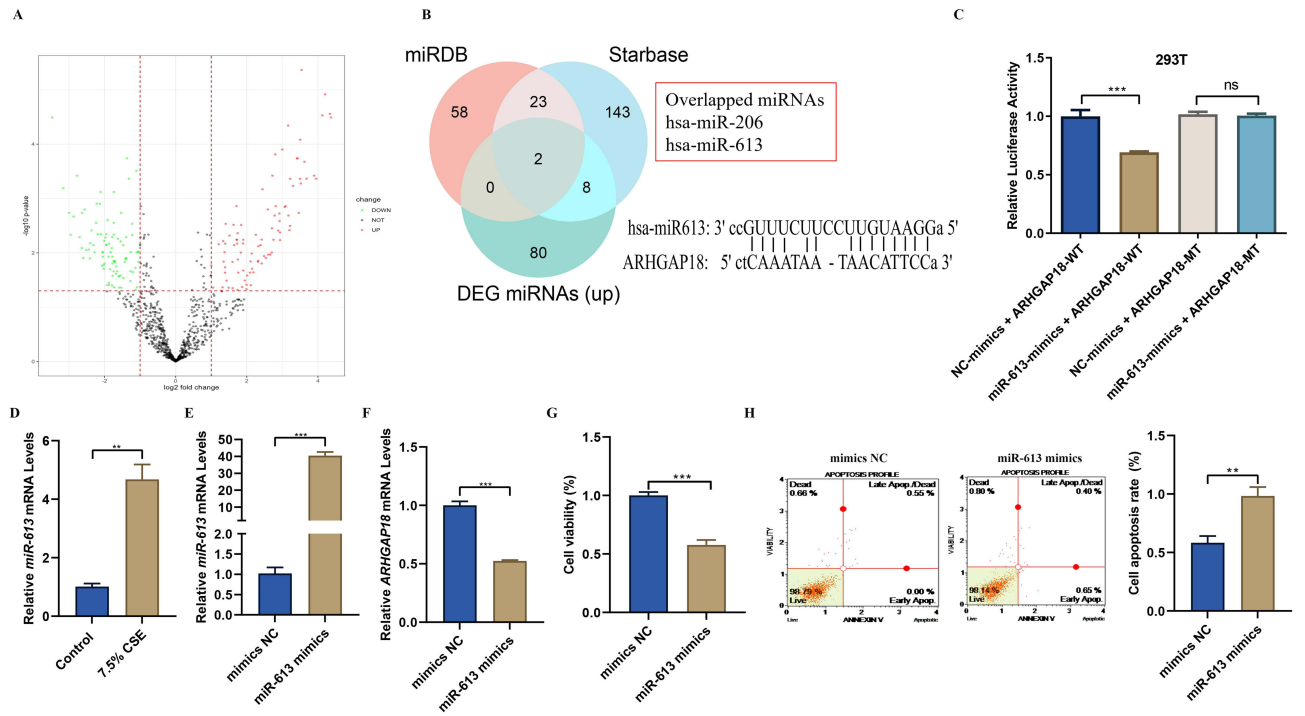

Figure 4 miR-613 mimics promoted cell apoptosis and inhibited proliferation and migration of BEAS-2B cells in vitro. (**A**) Volcano plot of differentially expressed miRNAs in COPD based on GSE24709 dataset (24 COPD and 19 controls). Red and blue dots represent up-regulated and downregulated genes, respectively. The gray dots indicate non-differentially expressed genes. The cutoff values were set as logFC> 1 or < −1 and adjusted *p*-value< 0.05. (**B**) Overlapped miRNAs of miRDB, Starbase, and differentially expressed miRNAs. (**C**) The targeting relationship between miR-613 and *ARHGAP18* was explored by dual luciferase reporter gene assay. (**D**) The expression of miR-613 was detected by qRT-PCR in CSE-induced BEAS-2B cells. (**E**) Overexpression efficiency of miR-613 in BEAS-2B cells was detected by qRT-PCR. (**F**) The impact of miR-613 mimics on *ARHGAP18* was determined by qRT-PCR. (**G** and **H**) Cell viability and apoptosis were investigated by CCK8 and flow cytometry. The results are presented as the mean ± SD of three independent experiments (n= 3). One-way ANOVA was applied for multi-group comparisons, with statistical significance set as $p< 0.05$. **: $p< 0.01$, and ***: $p< 0.0001$.

613 expression (Figure 4E) alongside a notable suppression of *ARHGAP18* (Figure 4F). In addition, miR-613 mimics significantly suppressed the proliferation of CSE-induced BEAS-2B cells (Figure 4G). Apoptosis assays further demonstrated that miR-613 mimics enhanced apoptosis in CSE-induced BEAS-2B (Figure 4H). After transfection with miR-613 mimics, E-cadherin was decreased, while N-cadherin and α-SMA were notably increased (Figure 5A). At the same time, IL-1β and TNF-α were also significantly upregulated (Figure 5B).

miR-613 Inhibits Inflammatory Response and Epithelial-Mesenchymal Transition in CSE-Treated BEAS-2B Cells by Promoting ARHGAP18

After transfection of the miR-613 inhibitor into BEAS-2B cells, the cell viability and migration ability were significantly enhanced (Figure 6A and C), and apoptosis was inhibited (Figure 6B). Rescue experiments showed that co-transfection of miR-613 inhibitor and siARHGAP18 in BEAS-2B cells could alleviate the effect of miR-613. Additionally, miR-613 inhibitor suppressed IL-1β and TNF-α levels, while co-transfection of miR-613 inhibitor and siARHGAP18 led to IL-1β and TNF-α's higher expression (Figure 6D). Moreover, miR-613 inhibitor enhanced E-cadherin and decreased N-cadherin and Vimentin; however, co-transfection of miR-613 inhibitor and siARHGAP18 decreased E-cadherin and enhanced N-cadherin and Vimentin (Figure 6E).

Discussion

COPD represents a significant global health challenge, affecting approximately 650 million people worldwide, and ranking as the third leading cause of death.[24] Despite advances in clinical management, current therapeutic options primarily focus on symptom relief and lung function improvement, with no medications proven to alter the progressive

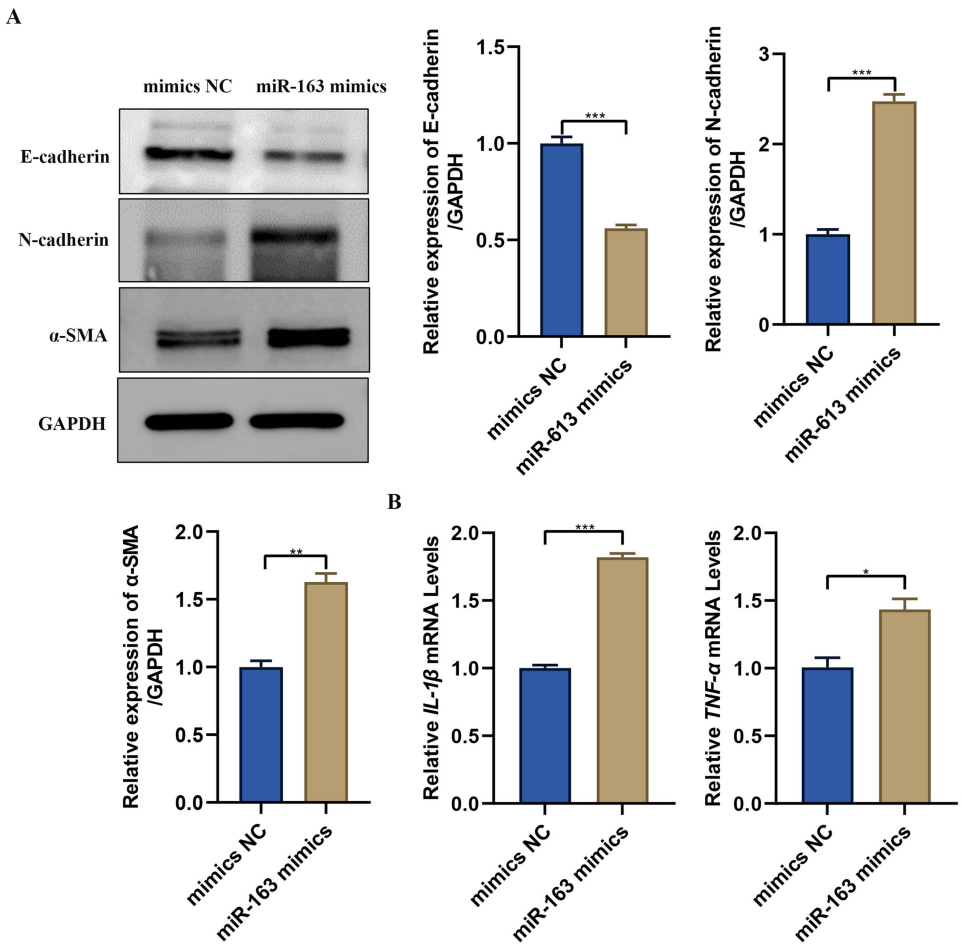

Figure 5 miR-613 mimics promoted EMT and inflammatory response. (**A**) The impact of miR-613 mimics on EMT-related protein levels was determined by Western blotting. (**B**) The levels of IL-1β and TNF-α were measured by qRT-PCR. The results are presented as the mean ± SD of three independent experiments (n= 3). One-way ANOVA was applied for multi-group comparisons, with statistical significance set as $p < 0.05$. *: $p< 0.05$, **: $p< 0.01$, and ***: $p< 0.0001$.

nature of the disease or reduce COPD-related mortality.[25] This therapeutic limitation underscores the urgent need for novel molecular targets and mechanistic insights into COPD pathogenesis.

From a clinical viewpoint, airway epithelial dysfunction emerges as a critical early event in the development of COPD and is closely correlated with exposure to cigarette smoke.[26] Epithelial cells not only constitute the primary defense barrier against inhaled toxic substances but also actively engage in the inflammatory responses and airway remodeling processes that are observed in patients with COPD. In this study, *ARHGAP18* was identified as a key gene closely related to epithelial dysfunction in COPD by integrating GSE datasets, scRNA-seq data, and three machine-learning methods. Further study showed that *ARHGAP18* has a central function in regulating apoptosis, proliferation, migration, and EMT of BEAS-2B cells induced by CSE, which gives new insight into the molecular mechanism of COPD progression.

Our study found that *ARHGAP18* was downregulated in CSE-treated BEAS-2B cells. The low expression of ARHGAP18 in CSE-induced BEAS-2B cells suggests that *ARHGAP18* may have a protective effect on COPD. Overexpression of ARHGAP18 significantly inhibited CSE-induced cell apoptosis, promoted cell proliferation and migration, and suppressed pro-inflammatory factors IL-1 β and TNF-α expressions. Our results align with previous studies demonstrating that RhoGAPs regulate cytoskeletal dynamics, cell adhesion, and inflammatory responses. For example, Xu et al showed that *ARHGAP18* could inhibit doxorubicin-induced RhoA activation, cell apoptosis, and ROS elevation in chronic heart failure.[27] Besides, Chen et al demonstrated that the upregulated ARHGAP18 increased the proliferation and invasion in hepatocellular carcinoma.[28] Moreover, Prins et al found that the decreased migration

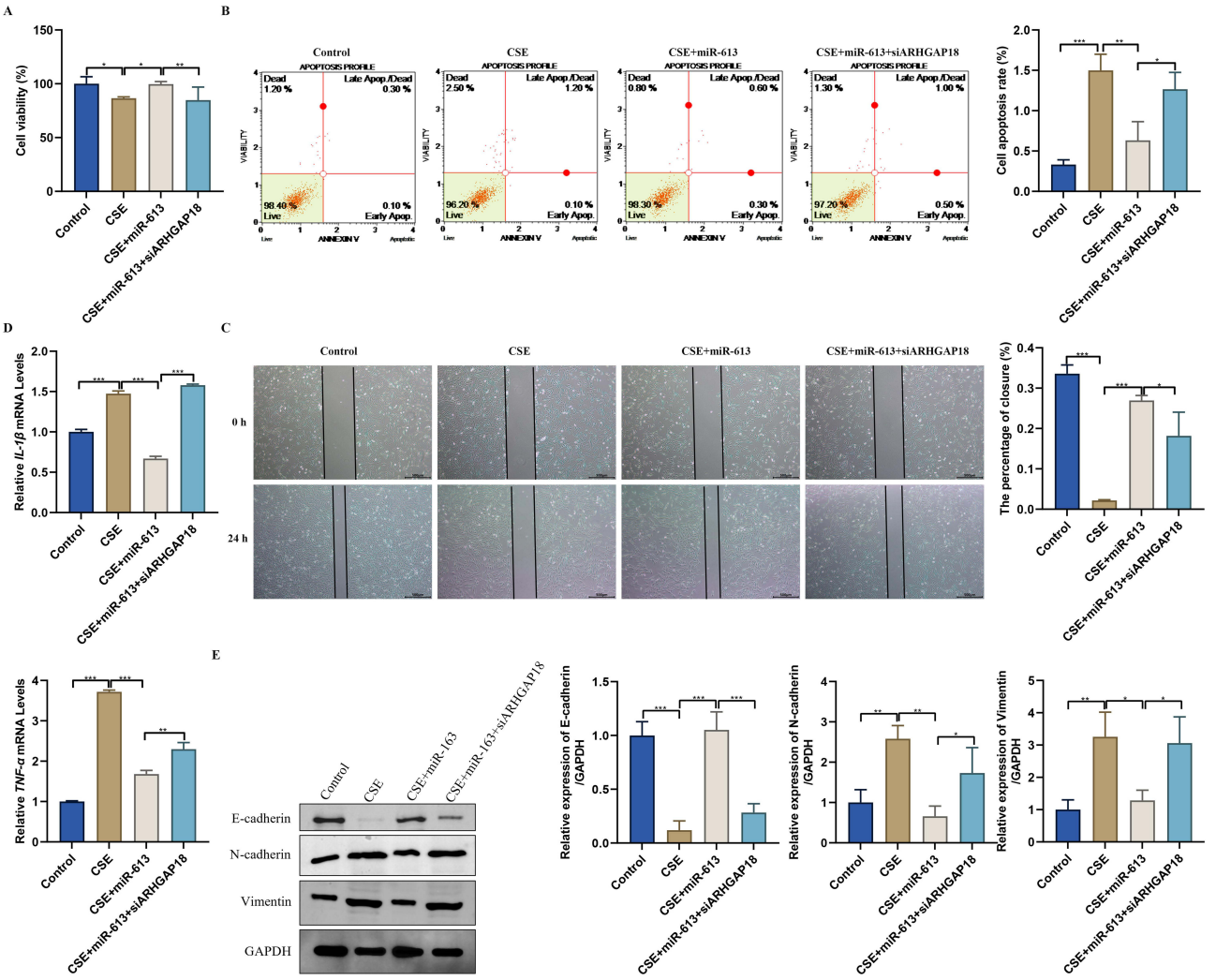

Figure 6 miRNA-613 alleviates EMT and inflammatory response by upregulating *ARHGAP18*. (**A–C**) Cell viability, apoptosis, and migration were determined by CCK8, flow cytometry, and wound healing assay in CSE-induced BEAS-2B cells. (**D**) qRT-PCR analysis of IL-1β and TNF-α in CSE-BEAS-2B cells. (**E**) Expression of EMT markers (E-cadherin, N-cadherin, and Vimentin) measured by Western blotting. The results are presented as the mean ± SD of three independent experiments (n= 3). One-way ANOVA was applied for multi-group comparisons, with statistical significance set as $p< 0.05$. *: $p< 0.05$, **: $p< 0.01$, and ***: $p< 0.0001$.

capacity of epithelial cells was associated with increased ARHGAP18 protein levels.[29] Taken above, *ARHGAP18* has a potential role in COPD pathogenesis by maintaining the integrity and function of epithelial cells under CS exposure. EMT, a process closely associated with airway remodeling and fibrosis in COPD, is marked by the downregulation of epithelial markers (E-cadherin) and the upregulation of mesenchymal markers (vimentin and fibronectin).[30] Wang et al demonstrated that *SMAD4* promotes EMT during CS-induced airway remodeling in COPD.[31] Besides, GLUT3 could regulate CSE-induced airway remodeling in COPD by influencing the NF-κB/ZEB1 pathway.[32] In our study, *ARHGAP18* overexpression elevated E-cadherin levels while suppressing the expression of N-cadherin and Vimentin. The above results suggest that *ARHGAP18* inhibits EMT, underscoring its potential therapeutic value in alleviating airway remodeling in COPD. In clinical practice, inhibiting EMT may help to reduce airway remodeling and improve the function of airways in COPD patients.

MiRNAs have received significant attention in the regulation of gene expression due to their critical role in cell differentiation, inflammation regulation, and fibrosis processes.[33–36] Our study found that miR-613 was the direct upstream regulator of *ARHGAP18* through bioinformatic analysis and luciferase reporter assays. miR-613 has been extensively studied in various cancers and inflammatory diseases. For example, Duan et al showed that miR-613 decreased the proliferation, invasion, and migration of renal cell carcinoma by regulating *AXL* levels.[17] Besides, miR-

613 could suppress papillary thyroid carcinoma progression by targeting *TAGLN2*.[18] Xiao et al revealed that miR-613 overexpression suppressed IL-1β-induced injury in osteoarthritis through decreasing fibronectin 1 expression.[37] However, the function of miR-613 in COPD has not been explored. We found that miR-613 negatively regulated *ARHGAP18* expression in CSE-induced BAS-2B cells. Inhibition of miR-613 mimicked the protective effects of *ARHGAP18* overexpression, including reduced apoptosis, enhanced proliferation, and migration, and suppressed expression of IL-1β and TNF-α, as well as inhibition of the EMT process. These results suggest that the miR-613/ARHGAP18 axis plays a critical role in the pathogenesis of COPD. Functional rescue experiments further confirmed that miR-613 regulates COPD progression by modulating *ARHGAP18* expression and the EMT process. This regulatory network establishes a mechanistic link between epigenetic regulation (miR-613) and cellular processes (*ARHGAP18*-mediated EMT) in COPD. Notably, a study by Zhou et al demonstrated that HOTAIR could suppress EMT in laryngeal squamous cell carcinoma by regulating the miR-613-SNAI2 axis,[38] further supporting the importance of miR-613 in EMT regulation. Targeting the miR-613/ARHGAP18 axis may offer a novel therapeutic strategy for COPD, particularly in patients with aberrant miR-613 expression. In clinical practice, this therapeutic strategy could be explored in patients with specific miR-613 expression profiles to achieve more targeted and effective treatment.

There are some limitations in our study. First, this study is mainly based on in vitro experiments of BEAS-2B cells, and it needs further verification in animal models and clinical samples. Second, the specific molecular mechanism of *ARHGAP18* regulating EMT and inflammation is still unclear, and further research on its downstream signaling pathway and interacting proteins is needed in the future. Despite its limitations, this study is the first to identify *ARHGAP18* as a key regulator of epithelial cell function in COPD and reveals the importance of the miR-613/ARHGAP18 axis as a potential therapeutic target. *ARHGAP18* plays various roles in the pathogenesis of COPD by regulating apoptosis, proliferation, migration, inflammatory reaction, and EMT. These findings deepen the understanding of COPD's molecular mechanisms and offer new directions for developing targeted therapy strategies to protect epithelial cell function. In the future, the clinical relevance of *ARHGAP18* and miR-613 in COPD patients should be further explored in large-scale clinical studies to confirm their potential as biomarkers and therapeutic targets. For example, evaluating the expression levels of *ARHGAP18* and miR-613 in COPD patients with different disease severities could help establish their correlation with disease progression and prognosis. Additionally, clinical trials targeting the miR-613/*ARHGAP18* axis could be designed to assess its safety and efficacy in COPD treatment.

Conclusion

In conclusion, our study was the first to explore the roles of *ARHGAP18* in COPD. We found that *ARHGAP18* was lowly expressed in CSE-induced BEAS-2B cells. *ARHGAP18* overexpression attenuated cell apoptosis, inflammatory response, and epithelial-mesenchymal transition of COPD in vitro. Typically, the molecular mechanism might be that miR-613 promoted COPD progression and EMT by directly regulating *ARHGAP18*. However, it should be noted that our findings are currently based on in vitro experiments. Therefore, further validation through animal experiments and clinical studies is essential to confirm the reliability and universality of these results, which will provide a more solid foundation for the development of novel therapeutic strategies targeting *ARHGAP18* and miR-613 in COPD.

Data Sharing Statement

Data are available from the corresponding author upon reasonable request.

Ethics Statement

Our study was approved by the Ethics Committee of the Hainan General Hospital.

Author Contributions

All authors made a significant contribution to the work reported, whether that is in the conception, study design, execution, acquisition of data, analysis and interpretation, or in all these areas; took part in drafting, revising or critically reviewing the article; gave final approval of the version to be published; have agreed on the journal to which the article has been submitted; and agree to be accountable for all aspects of the work.

Funding

This paper was supported by the Innovation Platform for Academicians of Hainan Province (No.YSPTZX202312), the Hainan Province Science and Technology Special Fund (No. ZDYF2024SHFZ094), the National Natural Science Foundation of China (No.82460010), and the Innovation Platform for Academicians of Hainan Province.

Disclosure

There are no conflicts of interest related to this study.

References

1. Christenson SA, Smith BM, Bafadhel M, Putcha N. Chronic obstructive pulmonary disease. *Lancet*. 2022;399(10342):2227–2242. doi:10.1016/S0140-6736(22)00470-6
2. Hurst JR, Siddiqui MK, Singh B, Varghese P, Holmgren U, de Nigris E. A systematic literature review of the humanistic burden of COPD. *International Journal of Chronic Obstructive Pulmonary Disease*. 2021;16:1303–1314. doi:10.2147/COPD.S296696
3. Halpin DM. Do the 'missing millions' of COPD patients want to be found? *Thorax*. 2023;78(6):531–532. doi:10.1136/thorax-2023-220113
4. Mao R, Liu Z, Zhao Y, et al. Stable Chronic Obstructive Pulmonary Disease (COPD) management under a tiered medical system in China. *Int J Chronic Obstruct Pulm Dis*. 2022;17:181–194. doi:10.2147/COPD.S333274
5. Xu J, Zeng Q, Li S, Su Q, Fan H. Inflammation mechanism and research progress of COPD. *Front Immunol*. 2024;15:1404615. doi:10.3389/fimmu.2024.1404615
6. Moll M, Silverman EK. Precision Approaches to Chronic Obstructive Pulmonary Disease Management. *Ann Rev Med*. 2024;75:247–262. doi:10.1146/annurev-med-060622-101239
7. Faruqi MA, Khan M, Mannino DM. Perspectives on ensifentrine and its therapeutic potential in the treatment of COPD: evidence to date. *Int J Chronic Obstruct Pulm Dis*. 2024;19:11–16. doi:10.2147/COPD.S385811
8. Milara J, Peiró T, Serrano A, Cortijo J. Epithelial to mesenchymal transition is increased in patients with COPD and induced by cigarette smoke. *Thorax*. 2013;68(5):410–420. doi:10.1136/thoraxjnl-2012-201761
9. Wei Y, Li Q, He K, et al. Mechanism of cigarette smoke in promoting small airway remodeling in mice via STAT 3 / PINK 1-Parkin / EMT. *Free Radical Biol Med*. 2024;224:447–456. doi:10.1016/j.freeradbiomed.2024.08.036
10. Li D, Shen C, Liu L, et al. PKM2 regulates cigarette smoke-induced airway inflammation and epithelial-to-mesenchymal transition via modulating PINK1/Parkin-mediated mitophagy. *Toxicology*. 2022;477:153251. doi:10.1016/j.tox.2022.153251
11. Ye R, Wang C, Sun P, Bai S, Zhao L. AGR3 regulates airway epithelial junctions in patients with frequent exacerbations of COPD. *Front Pharmacol*. 2021;12:669403. doi:10.3389/fphar.2021.669403
12. Zhang Z, Lin F, Liu F, et al. Proteomic profiling reveals a distinctive molecular signature for critically ill COVID-19 patients compared with asthma and chronic obstructive pulmonary disease. *Int J Infect Dis*. 2022;116:258–267. doi:10.1016/j.ijid.2022.01.008
13. Lombardo AT, Mitchell CAR, Zaman R, McDermitt DJ, Bretscher A. ARHGAP18-ezrin functions as an autoregulatory module for RhoA in the assembly of distinct actin-based structures. *eLife*. 2024;13. doi:10.7554/eLife.83526
14. Coleman PR, Lay AJ, Ting KK, et al. YAP and the RhoC regulator ARHGAP18, are required to mediate flow-dependent endothelial cell alignment. *Cell Commun Signal*. 2020;18(1):18. doi:10.1186/s12964-020-0511-7
15. Santos JMO, Peixoto da Silva S, Gil da Costa RM, Medeiros R. The emerging role of MicroRNAs and other non-coding RNAs in cancer Cachexia. *Cancers*. 2020;12(4):1004. doi:10.3390/cancers12041004
16. Chen M, Zhang J, Huang H, Wang Z, Gao Y. miRNA-206-3p alleviates LPS-induced acute lung injury via inhibiting inflammation and pyroptosis through modulating TLR4/NF-κB/NLRP3 pathway. *Sci Rep*. 2024;14(1):11860. doi:10.1038/s41598-024-62733-5
17. Duan W, Pan S, Zhai Y, et al. miR-613 suppresses renal cell carcinoma proliferation, invasion and migration by regulating the AXL/AKT pathway. *Exp Biol Med*. 2023;248(4):281–292. doi:10.1177/15353702231151962
18. Huang Y, Zhang H, Wang L, et al. MiR-613 inhibits the proliferation, migration, and invasion of papillary thyroid carcinoma cells by directly targeting TAGLN2. *Cancer Cell Int*. 2021;21(1):494. doi:10.1186/s12935-021-02083-8
19. Liu C, Jiang Y. miR-613 suppresses chemoresistance and stemness in triple-negative breast cancer by targeting FAM83A. *Cancer Manag Res*. 2020;12:12623–12633. doi:10.2147/CMAR.S276316
20. Wan J, Liu S. miR-613 inhibits the proliferation of human ovarian granulosa cells by arresting cell cycle progression via the targeting of IGF-1. *Mol Med Rep*. 2021;23(3).
21. Yang M, Zhou W, Xu M, et al. Tumor suppressor miR-613 alleviates non-small cell lung cancer cell via repressing M2 macrophage polarization. *J Oncol*. 2023;2023:2311231. doi:10.1155/2023/2311231
22. Zhang M, Tang J, Shan H, et al. p66Shc mediates mitochondrial dysfunction dependent on PKC activation in airway epithelial cells induced by cigarette smoke. *Oxid Med Cell Longevity*. 2018;2018:5837123. doi:10.1155/2018/5837123
23. Xian M, Xu J, Zheng Y, et al. Network pharmacology and experimental verification reveal the regulatory mechanism of chuanbeimu in treating chronic obstructive pulmonary disease. *Int J Chron Obstruct Pulmon Dis*. 2024;19:799–813. doi:10.2147/COPD.S442191
24. Mathioudakis AG, Janssens W, Sivapalan P, et al. Acute exacerbations of chronic obstructive pulmonary disease: in search of diagnostic biomarkers and treatable traits. *Thorax*. 2020;75(6):520–527. doi:10.1136/thoraxjnl-2019-214484
25. Barnes PJ, Baker J, Donnelly LE. Cellular senescence as a mechanism and target in chronic lung diseases. *Am J Respir Crit Care Med*. 2019;200(5):556–564. doi:10.1164/rccm.201810-1975TR
26. Gao W, Li L, Wang Y, et al. Bronchial epithelial cells: the key effector cells in the pathogenesis of chronic obstructive pulmonary disease? *Respirology*. 2015;20(5):722–729. doi:10.1111/resp.12542
27. Xu Z, Hu Z, Xu H, et al. Liquiritigenin alleviates doxorubicin-induced chronic heart failure via promoting ARHGAP18 and suppressing RhoA/ROCK1 pathway. *Exp Cell Res*. 2022;411(2):113008. doi:10.1016/j.yexcr.2022.113008

28. Chen P, Liu X, Liu Y, Bao X, Wu Q. ARHGAP18 is Upregulated by Transcription Factor GATA1 Promotes the Proliferation and Invasion in Hepatocellular Carcinoma. *Appl Biochem Biotechnol*. 2024;196(2):679–689. doi:10.1007/s12010-023-04459-0
29. Prins MMC, Giugliano FP, van Roest M, van de Graaf SFJ, Koelink PJ, Wildenberg ME. Thiopurines correct the effects of autophagy impairment on intestinal healing - a potential role for ARHGAP18/RhoA. *Dis Mod Mech*. 2021;14(4). doi:10.1242/dmm.047233
30. Shukla S, Ward C, Walters EH. Mechanistic insights on EMT and smoking-related COPD. *Stem Cell Rev Rep*. 2021;17(4):1503–1504. doi:10.1007/s12015-021-10152-8
31. Wang Z, Ding Y, Wang P, et al. SMAD4 promotes EMT in COPD airway remodeling induced by cigarette smoke through interaction with O-GlcNAc transferase. *Ecotoxicol Environ Saf*. 2024;284:116931. doi:10.1016/j.ecoenv.2024.116931
32. Ding Y, Wang Z, Zhang Z, You R, Wu Y, Bian T. GLUT3-mediated cigarette smoke-induced epithelial-mesenchymal transition in chronic obstructive pulmonary disease through the NF-kB/ZEB1 pathway. *Respir Res*. 2024;25(1):158. doi:10.1186/s12931-024-02785-3
33. Xie J, Du Y, Liu D, et al. The miR-17~92 miRNAs promote plasma cell differentiation by suppressing SOCS3-mediated NIK degradation. *Cell Rep*. 2023;42(8):112968. doi:10.1016/j.celrep.2023.112968
34. Iantomasi T, Romagnoli C, Palmini G, et al. Oxidative stress and inflammation in osteoporosis: molecular mechanisms involved and the relationship with microRNAs. *Int J Mol Sci*. 2023;24(4):3772. doi:10.3390/ijms24043772
35. Liu Y, Zhang Z, Wang B, et al. Inflammation-stimulated MSC-derived small extracellular vesicle miR-27b-3p regulates macrophages by targeting CSF-1 to promote temporomandibular joint condylar regeneration. *Small*. 2022;18(16):e2107354. doi:10.1002/smll.202107354
36. Yang H, Wang W, Xiao J, et al. ROS-responsive injectable hydrogels loaded with exosomes carrying miR-4500 reverse liver fibrosis. *Biomaterials*. 2025;314:122887. doi:10.1016/j.biomaterials.2024.122887
37. Xiao P, Zhu X, Sun J, et al. MicroRNA-613 alleviates IL-1β-induced injury in chondrogenic CHON-001 cells by targeting fibronectin 1. *Am J Transl Res*. 2020;12(9):5308–5319.
38. Zhou JC, Zhang JJ, Ma W, et al. Anti-tumor effect of HOTAIR-miR-613-SNAI2 axis through suppressing EMT and drug resistance in laryngeal squamous cell carcinoma. *RSC Adv*. 2018;8(52):29879–29889. doi:10.1039/C8RA04514C